

A Novel in-Band OSNR Measurement Method Based on Normalized Autocorrelation Function

Volume 10, Number 2, April 2018

Zhuili Huang

Jifang Qiu, *Member, IEEE*

Deming Kong, *Member, IEEE*

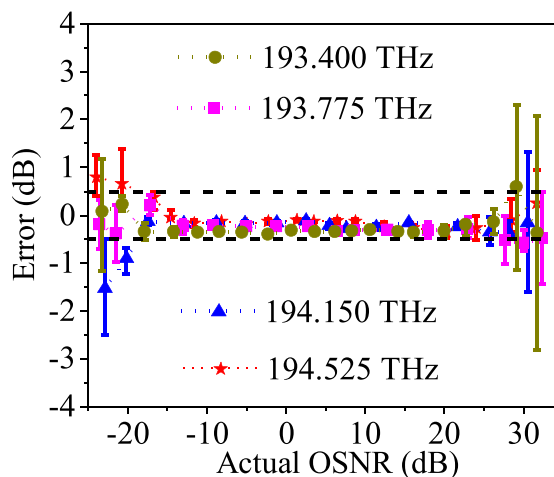
Ye Tian

Yan Li, *Member, IEEE*

Hongxiang Guo

Xiaobin Hong

Jian Wu, *Member, IEEE*



DOI: 10.1109/JPHOT.2017.2717847

1943-0655 © 2017 IEEE

A Novel in-Band OSNR Measurement Method Based on Normalized Autocorrelation Function

Zhuili Huang, Jifang Qiu, *Member, IEEE*,
Deming Kong, *Member, IEEE*, Ye Tian, Yan Li, *Member, IEEE*,
Hongxiang Guo, Xiaobin Hong, and Jian Wu, *Member, IEEE*

State Key Laboratory of Information Photonics and Optical Communications, Beijing
University of Posts and Telecommunications, Beijing 100876, China

DOI:10.1109/JPHOT.2017.2717847
1943-0655 © 2017 IEEE

Manuscript received May 9, 2017; revised June 11, 2017; accepted June 16, 2017. Date of publication June 21, 2017; date of current version April 19, 2017. This work was supported by the 863 Program 2013AA014202, 973 Program 2014CB340100, and NSFC Programs 61205031, 61307055, 61335009, 61505011, and 61475022. Corresponding author: Jifang Qiu (e-mail: jifangqiu@bupt.edu.cn).

Abstract: We propose and experimentally demonstrate a novel in-band optical signal-to-noise ratio (OSNR) measurement method based on normalized autocorrelation function. Experimental results indicate that OSNR of four-channel 32-Gbaud pulse-duration modulation-QPSK wavelength-division-multiplexing signals is precisely measured with applicability to flexible channel spacing. The measurement range is 37 dB from -15 to 22 dB with error less than ± 0.5 dB. The proposed method is also robust to bit rate, modulation format, chromatic dispersion, and input optical power. Besides, the choice of delay in calculation of normalized autocorrelation function is flexible from 1.6 to 30 ps.

Index Terms: Flexible channel spacing, normalized autocorrelation function, optical signal to noise ratio (OSNR), Wiener–Khinchin theorem.

1. Introduction

Optical performance monitoring (OPM) has received much attention in helping maintaining proper system operation and fault management [1]. Among various optical performance monitoring parameters, optical signal to noise ratio (OSNR) is a key performance indicator of transmission link quality, therefore needs to be accurately measured [2]. However, traditional out-band OSNR monitoring method, where the level of amplified spontaneous emission (ASE) noise at carrier wavelength is measured by interpolating the noise level from spectral gaps between signals, tends to be inaccurate for WDM systems with ultra-narrow channel space, or dynamic WDM networks with optical add-drop modules (OADM). To alleviate this challenge, several in-band OSNR monitoring techniques have been proposed, which are based on different working principles. The polarization-nulling method [3] is based on the different polarization characteristics of ASE noises and signal. However, it is not practical for the real optical fiber transmission system with polarization mode dispersion (PMD) and polarization dependent loss (PDL). Interferometry [4]–[8] measures the constructive and destructive optical power of output ports of interferometer to determine the OSNR. Waveform sampling method [9], [10] is on the basis of extracting parameters in the sampling histogram plots. The method using intensity autocorrelations of data streams [11] depends on the instantaneous optical intensity, which is sensitive to chromatic dispersion (CD). And the basis for

the approaches based on nonlinear effects [12]–[14] is the dependence of the power from nonlinear effects on the OSNR.

On the other hand, to improve the capacity of optical transport network, advanced modulation format, such as M-PSK and 16-QAM [15], and wavelength-division multiplexed (WDM) technique are adopted. Besides, considering the flexibility of network, the modulation format and bit rate of different carrier signals are different. Therefore, OSNR measurement methods are required to be compatible with different modulation formats and bit rates in WDM system with narrow channel spacing.

In this paper, we propose and experimentally demonstrate a novel in-band optical signal-to-noise ratio measurement method based on normalized autocorrelation function with ultra-large measurement range, which is insensitive to CD and input optical power. Plus, it has advantages of simple setup, convenient operation and easy maintenance. Experimental results show that OSNR measurement for 4-channel 32 Gbaud PDM-QPSK WDM signals works well from -15 to 22 dB with error less than ± 0.5 dB. Besides, robustness of bit rate and modulation format indicates that the method is compatible with flexible WDM system with different modulation formats and bit rates.

2. Principle of Operation

Before explaining the operation principle, it is necessary to clear out three important symbols used throughout the paper, i.e., ns , s and n , which represent noisy signal (signal degraded by noise, which needs to be OSNR measured), signal (noise-free signal), and noise (signal-free noise).

According to the Wiener–Khinchin theorem [16], autocorrelation function (ACF) and power spectral density are Fourier Transform pairs as Eq. (1).

$$R_i(\tau) = \int F_i(f) e^{j2\pi f\tau} df \quad (1)$$

where $F_i(f)$ and $R_i(\tau)$ stand for the power spectral density and ACF of noise ($i = n$) /signal ($i = s$) /noisy signal ($i = ns$), respectively. While, average optical power P_i is expressed as

$$P_i = R_i(0) = \int_{-\infty}^{+\infty} F_i(f) df \quad (2)$$

Therefore, the normalized autocorrelation function (NACF), $\gamma_i(\tau)$, can be expressed as

$$\gamma_i(\tau) = R_i(\tau)/R_i(0) = R_i(\tau)/P_i \quad (3)$$

For noisy signal, taking into account $F_{ns}(f) = F_s(f) + F_n(f)$ and $P_{ns} = P_s + P_n$, $\gamma_{ns}(\tau)$ can be expressed from Eq. (3) as

$$\gamma_{ns}(\tau) = \frac{\gamma_n(\tau)P_n + \gamma_s(\tau)P_s}{P_s + P_n} = \frac{\gamma_n(\tau) + \gamma_s(\tau)P_s/P_n}{1 + P_s/P_n} \quad (4)$$

Then for a fixed delay τ_0

$$r \equiv P_s/P_n = \frac{\gamma_n(\tau_0) - \gamma_{ns}(\tau_0)}{\gamma_{ns}(\tau_0) - \gamma_s(\tau_0)} \quad (5)$$

According to Eq. (5) and the definition of OSNR, we can obtain the OSNR of noisy signal as

$$\begin{aligned} OSNR &= 10 \log_{10} \left(r \cdot \frac{NEB}{0.1(nm)} \right) \\ &= 10 \log_{10} \left(\frac{\gamma_n(\tau_0) - \gamma_{ns}(\tau_0)}{\gamma_{ns}(\tau_0) - \gamma_s(\tau_0)} \right) + 10 \log_{10} \left(\frac{NEB}{0.1(nm)} \right) \end{aligned} \quad (6)$$

where NEB is the noise equivalent bandwidth of channel filter. $\gamma_n(\tau_0)$ and $\gamma_s(\tau_0)$, which are independent of OSNR, can be considered as initial constants. Therefore, OSNR can be calculated from Eq. (6) when the power spectral density of noisy signal, $F_{ns}(f)$, is obtained. Due to the fact that $\gamma_i(\tau_0)$, ($i = n, s$ and ns) is only dependent on the shape of optical power spectrum, is independent

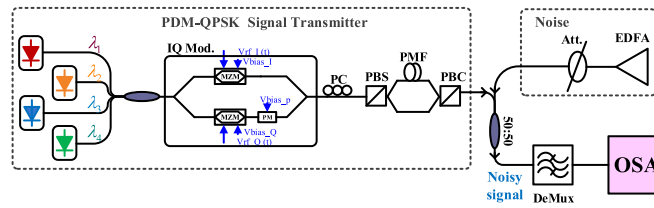


Fig. 1. Experimental setup for OSNR measurement in a WDM system with 37.5-GHz channel spacing. PC: polarization controller, PMF: polarization maintaining fiber, PBS: polarization beam splitter, PBC: polarization beam combiner; OSA: optical spectrum analyzer.

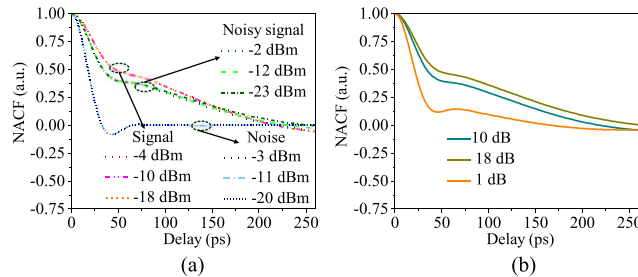


Fig. 2. NACFs of 32 Gbaud PDM-QPSK signal, noise and noisy signal after 37.5-GHz bandwidth filter with (a) different powers. (b) different OSNRs.

to the input optical power and the chromatic dispersion (CD) of transmission fiber, theoretically the proposed OSNR measurement method is robust to the variation of input optical power and CD of transmission link.

3. Experimental Setup and Results

3.1 Experimental Setup

The proposed method is demonstrated in an experimental setup shown in Fig. 1. Four continuous wave (CW) lights with 100-kHz linewidth, separated by channel spacing of 37.5 GHz, are combined by polarization maintaining couplers and modulated by an IQ modulator, which is driven by two independent 10/25/32 Gb/s pseudo-random binary sequence (PRBS) with lengths of $2^{11} - 1$ and $2^{15} - 1$ respectively, to generate 10/25/32 Gbaud QPSK signal. Then, the modulated signals are split, delayed and combined to generate noise-free polarization-division-multiplexed QPSK (PDM-QPSK) signals. An EDFA is used as an ASE noise source, output optical power of which is controlled by an attenuator after the EDFA. Next, the noise-free PDM-QPSK signals are combined with the differently attenuated ASE noise via a 3 dB fiber coupler to generate noisy signals with determined OSNR. After the WDM demultiplexer (with 37.5/50/100/200-GHz bandwidth of channel filter), the noisy signals are sent into an optical spectrum analyzer (OSA) for measuring the optical spectrum, which is used for calculation of its NACF by inverse fast Fourier transform (IFFT) method and normalization as shown in Eqs. (1) and (3). By turning off the CW laser (EDFA), the optical spectrum of signal-free noise (noise-free signal) is recorded to calculate $\gamma_n(\tau_0)$ ($\gamma_s(\tau_0)$) as initial constants.

3.2 Normalized Autocorrelation Function

The NACFs of signal (32 Gbaud PDM-QPSK), noise and noisy signal ($\gamma_i(\tau)$, $i = s, n, ns$) after 37.5-GHz bandwidth of filter with different optical power are shown in Fig. 2(a) respectively, where the NACFs of noise with optical power of -3 dBm, -11 dBm, and -20 dBm are superimposed, similar results are also obtained for noise-free signals and noisy signals with different optical powers, which indicate that the NACF is independent on optical power. On the other hand, for 1.6-100 ps,

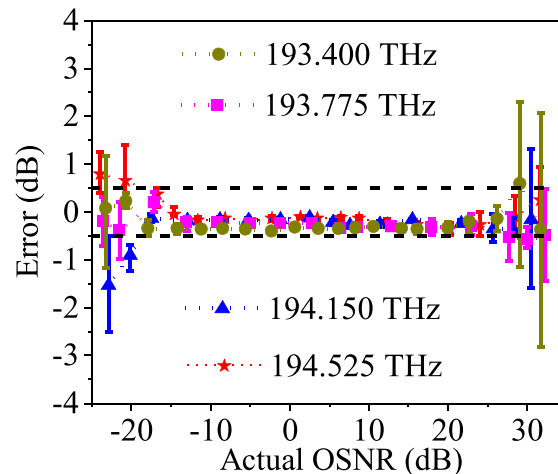


Fig. 3. OSNR measurement error versus actual OSNR for 4-channel 32 Gbaud PDM-QPSK WDM signals after 37.5-GHz bandwidth of filter.

$\gamma_{ns}(\tau)$ at different OSNRs of 1 dB, 10 dB and 18 dB are different as shown in Fig. 2(b), indicating that $\gamma_{ns}(\tau)$ is dependent on OSNR [17]. Therefore, based on $\gamma_{ns}(\tau)$ and Eq. (6), OSNR can be calculated.

3.3 WDM System

Then, we experimentally demonstrated the proposed OSNR measurement method in a 4-channel WDM system. Note that: 1. the actual OSNR was measured with signal on/off method [18]; 2. the modulation format of signal is 32 Gbaud-PDM-QPSK; 3. the bandwidth of channel filter is 37.5 GHz; 4. the sensitivity, sampling points, resolution and sampling range of OSA to obtain spectra is set as High1, 5001, 0.02 nm and 5 nm; 5. the delay of the NACFs are set at 3.2 ps; 6. every OSNR measurement was repeated 5 times; 7. the short lines and the points stand for the deviation range and mean value of OSNR measurement errors respectively throughout the paper without special notification. The OSNR errors (measured OSNR minus actual OSNR) versus actual OSNR for all 4 channels are shown in Fig. 3, where it can be seen that OSNR measurement error is kept less than ± 0.5 dB from -15 dB to 22 dB for 4 channels. Besides, when the error range expands to ± 1 dB, which is acceptable, the measurement range of this technique is up to 44 dB from -17 dB to 27 dB, which meets the requirement of optical communication system with complex modulation format. Therefore, it can be concluded that the method works well in WDM systems with 37.5 GHz channel spacing.

Next, we investigated the robustness of the proposed method under various conditions by changing the bandwidth of channel filter, baud rate and modulation format of signal, input optical power, by adding different amount of chromatic dispersion and by changing delay time τ in NACFs and. The details of experimental results are as follows. Note that only one channel is used during these investigations.

3.4 Bandwidth of Channel Filter

Firstly, as we know, the built-in OSNR measurement modular of OSA is based on linearly interpolating method, which tends to be inaccurate with narrow channel spacing as shown in Fig. 4(a) where the accuracy of the measured OSNR is dependent on the bandwidth of channel filter. When the filter bandwidth is 100 GHz, the valid OSNR measurement range is 10 dB to 20 dB with error less than ± 0.5 dB. When the filter bandwidth is 200 GHz or wider, the OSNR measurement range is 5 dB to 25 dB with error less than ± 0.5 dB. However, when the bandwidth is 50 GHz or narrower, the measurement errors increase significantly because the level of out-band noise is far less than

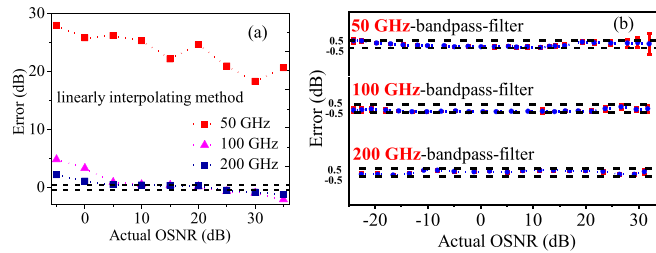


Fig. 4. OSNR error measured for 32 Gbaud PDM-QPSK signal under different bandwidths of filter based on (a) linearly interpolating method (b) normalized autocorrelation function.

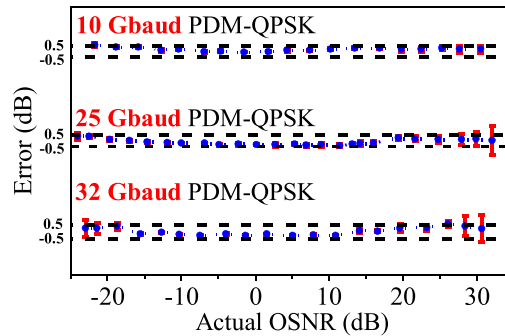


Fig. 5. OSNR measurement error for PDM-QPSK signals after 37.5 GHz filter with different baud rate.

the level of in-band noise with narrow channel filter. Meanwhile, the proposed method is valid with various channel spacing as shown in Fig. 4(b). When the filter bandwidth is set as 50 GHz, the OSNR measurement range is 45 dB from -20 dB to 25 dB. When the bandwidth of filter is 100 GHz and 200 GHz respectively, the OSNR measurement range is up to 50 dB from -20 dB to 30 dB. According to Fig. 3 and Fig. 4(b), we can see that the OSNR measurement method based on NACF can be applied on flexible channel spacing WDM system and the OSNR can be effectively measured when the channel spacing is as narrow as 37.5 GHz.

3.5 Baud Rate of Signal

Secondly, we changed the baud rate of signal from 10 to 25 to 32 Gbaud, and maintained the bandwidth of filter at 37.5 GHz. The experimental results are shown in Fig. 5, in which the OSNR measurement range is -20 to 30 dB for 10 Gbaud signal, -20 to 27 dB for 25 Gbaud signal, and -15 to 22 dB for 32 Gbaud signal with error less than ± 0.5 dB. During the OSNR range of -15 to 22 dB, the measurement error is kept less than ± 0.5 dB for 10, 25 and 32 Gbaud signal respectively. Consequently, it can be concluded that the OSNR measurement method is robust to baud rate of signal.

3.6 Modulation Format of Signal

Due to the limited experimental condition, a numerical simulation was carried out to investigate the applicability of proposed method on PDM-16 QAM signal. The bandwidth of channel filter was fixed at 37.5 GHz. Simulation results are shown in Fig. 6, where we can see that the valid OSNR measurement ranges are 40 dB from -8 to 32 dB and with error less than ± 0.5 dB. It can be seen that the proposed method has potential to be robust to the modulation format of signal.

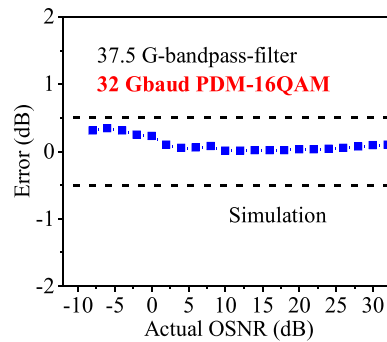


Fig. 6. Simulated OSNR measurement error for 32 Gbaud PDM-16-QAM signal after 37.5 GHz filter.

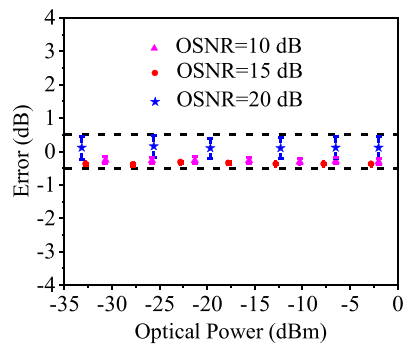


Fig. 7. OSNR measurement error versus input optical power for 32 Gbaud PDM-QPSK signal after 37.5 GHz filter.

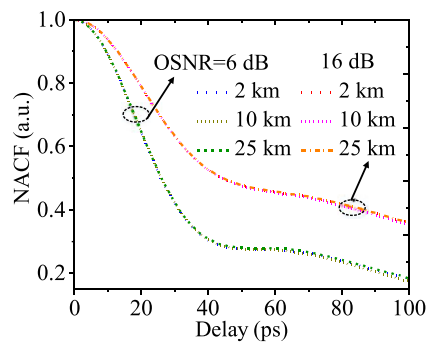


Fig. 8. NACF of noisy signal after transmission on SMF.

3.7 Optical Power

Then, we changed the input optical power of the noisy signal from -33 to -2 dBm when the OSNR is set as 10 dB, 15 dB and 20 dB respectively. The experimental results are shown in Fig. 7, where the variation of the measurement error is ignorable for different input powers, which means that the method is insensitive to input optical power.

3.8 Chromatic Dispersion

Next, we added different amounts of CD into the noisy signal by using different lengths of single mode fibers (SMFs). The measured and calculated $\gamma_{ns}(\tau)$ after propagating in single mode fibers (SMFs) with lengths from 2 km to 25 km are shown in Fig. 8. The results that $\gamma_{ns}(\tau)$ of the noisy

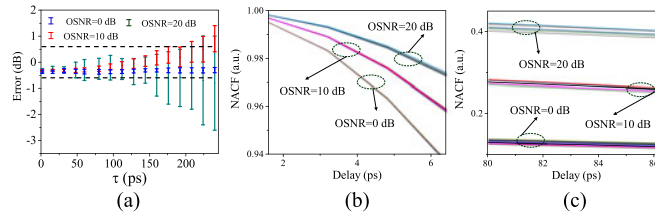


Fig. 9. (a) OSNR measurement error versus delay τ_0 of NACF in case of different OSNR; (b) NACFs of noisy signal versus delay for 128 Gb/s PDM-QPSK signal in case of different OSNR when the range of delay is 1.6-6.4 ps; (c) NACFs of noisy signal versus delay for 128 Gb/s PDM-QPSK signal in case of different OSNR when the range of delay is 80-86.4 ps.

signals with different amounts of CD but with same OSNR are superimposed indicate that the method is insensitive to CD.

3.9 Delay of NACF

At last, as the delay τ_0 of NACF in the proposed measurement method is a key parameter in OSNR calculation in (6), which determines the OSNR measurement performance to a certain degree, the OSNR measurements were repeated by 10 times here for stronger robustness. The effect on the accuracy of OSNR measurement was evaluated by experiments in which τ_0 was changed from 1.6 to 240 ps and the experimental results are shown in Fig. 9(a). It can be seen that the deviation of error increases as τ_0 rises because variation of γ_{ns} caused by ambient change increases with the increasing delay. In order to keep OSNR measurement error less than ± 0.5 dB, τ_0 needs to be set in ranges of 1.6-240 ps, 1.6-160 ps, and 1.6-30 ps for OSNR of 0 dB, 10 dB and 20 dB, respectively. Considering OSNR measurement range, the optional range of τ_0 is from 1.6 to 30 ps. We noticed that in Fig. 2, the NACFs seem almost coincident in small delay because the range of delay is set from 0 to 260 ps. Then we change the range of delay as 1.6 to 6.4 ps for more details in small delay, and NACFs of noisy signal versus delay, which are measured 10 times for each OSNR, are shown in Fig. 9(b). It can be seen that $\gamma_{ns}(\tau)$ of different OSNR are near, but different and stable. Fig. 9(c) shows the same NACFs of noisy signal versus delay when range of delay is 80-86.4 ps where the variation of $\gamma_{ns}(\tau)$ is much larger than Fig. 9(b). It can be concluded that the $\gamma_{ns}(\tau)$ in small delay is more insensitive to ambient change. Therefore, the accurate estimation can be obtained in small delay. In particular, delay = 0 ps is a singularity point where $\gamma_{ns} = \gamma_s = \gamma_n = 1$, which cannot be used in OSNR calculation.

4. Conclusion

We proposed and experimentally demonstrated a novel in-band OSNR measurement method based on normalized autocorrelation function. Experimental results of OSNR measurements for 4-channel 32 Gbaud PDM-QPSK signals indicate that the method works well in WDM systems with bandwidth of channel filter as narrow as 37.5 GHz, and has ultra-large measurement range from -15 dB to 22 dB with error less than ± 0.5 dB. Experimental results also show the robustness of this method to bandwidth of channel filter, baud rate, input optical power of the noisy signal and CD of transmission fiber. Additional simulation results show that this method has potential to be robust to the modulation format of signal. We noticed that for real system, it is possible to turn off the signal and measure the spectrum of the noise after Demux to calculate $\gamma_n(\tau_0)$, because NACF is only depend on the shape of spectrum, not depend on the level of power. But it is difficult to turn off the noise to measure the spectrum of noise-free signal because in a long optical link the fiber amplifiers have to be there so the signal will always accumulate additional noise. For this reason, it is difficult to obtain $\gamma_s(\tau)$. But there are two solutions about it. 1. the spectrum of signal can be obtained at transmitter to calculate $\gamma_s(\tau)$ because the shape of signal spectrum at transmitter is almost same as the shape at receiver

due to the fact that attenuation and CD have no effect on the shape of signal spectrum. However, it is undeniable that fiber nonlinearity causes spectral distortion, which may degrade the OSNR measurement performance of proposed method, but in communication system, spectral distortion caused by fiber nonlinearity is relatively slight. 2. $\gamma_s(\tau)$ can be expanded as $\gamma_s(\tau) = 1 - c\tau^2$, and by introducing different time delays of $\gamma_n(\tau_0)$ and $\gamma_{ns}(\tau_0)$, the OSNR can be calculated without prior knowledge of $\gamma_s(\tau)$ [5]. We will work on it to demonstrate the validity.

References

- [1] D. C. Kilper *et al.*, "Optical performance monitoring," *J. Lightw. Technol.*, vol. 22, no. 1, pp. 294–304, Jan. 2004.
- [2] Z. Pan, C. Yu, and A. E. Willner, "Optical performance monitoring for the next generation optical communication networks," *Opt. Fiber Technol.*, vol. 16, no. 1, pp. 20–45, 2010.
- [3] J. H. Lee, H. Y. Choi, S. K. Shin, and Y. C. Chung, "A review of the polarization-nulling technique for monitoring optical-signal-to-noise ratio in dynamic WDM networks," *IEEE J. Lightw. Technol.*, vol. 24, no. 11, pp. 4162–4171, Nov. 2006.
- [4] Z. N. Tao, Z. Y. Chen, L. B. Fu, D. M. Wu, and A. S. Xu, "Monitoring of OSNR by using a Mach-Zehnder interferometer," *Microw. Opt. Technol. Lett.*, vol. 30, no. 1, pp. 63–65, Jul. 2001.
- [5] E. Flood *et al.*, "In-band OSNR monitoring using a pair of Michelson fiber interferometers," *Opt. Exp.*, vol. 18, no. 4, pp. 3618–3625, 2010.
- [6] M. R. Chitgarha *et al.*, "Demonstration of in-service wavelength division multiplexing optical-signal-to-noise ratio performance monitoring and operating guidelines for coherent data channels with different modulation formats and various baud rates," *Opt. Lett.*, vol. 39, no. 6, pp. 1605–1608, 2014.
- [7] M. Nakajima, N. Nemoto, K. Yamaguichi, J. Yamaguchi, K. Suzuki, and T. Hashimoto, "In-band OSNR monitors comprising programmable delay line interferometer integrated with wavelength selective switch by spatial and planar optical circuit," presented at the Opt. Fiber Commun. Conf., Anaheim, CA, USA, 2016, Paper Th2A.11.
- [8] J. Qiu, Z. Huang, B. Yuan, N. An, D. Kong, and J. Wu, "Multi-wavelength in-band OSNR monitor based on Lyot-Sagnac interferometer," *Opt. Exp.*, vol. 23, no. 16, pp. 20257–20266, 2015.
- [9] I. Shake and H. Takara, "Averaged Q-factor method using amplitude histogram evaluation for transparent monitoring of optical signal-to-noise ratio degradation in optical transmission system," *IEEE J. Lightw. Technol.*, vol. 20, no. 8, pp. 1367–1373, Aug. 2002.
- [10] Y. Yu, B. Zhang, and C. Yu, "Optical signal to noise ratio monitoring using single channel sampling technique," *Opt. Exp.*, vol. 22, no. 6, pp. 6874–6880, 2014.
- [11] M. Dinu, C. K. Daniel, and R. S. Howard, "Optical performance monitoring using data stream intensity autocorrelation," *J. Lightw. Technol.*, vol. 24, no. 3, pp. 1194–1202, Mar. 2006.
- [12] M. D. Pelusi, A. Fu, and B. J. Eggleton, "Multi-channel in-band OSNR monitoring using stimulated Brillouin scattering," *Opt. Exp.*, vol. 18, no. 9, pp. 9435–9446, Apr. 2010.
- [13] J. Y. Huh and Y. C. Chung, "Simultaneous monitoring technique for OSNR and PMD based on four-wave mixing in SOA," presented at the Opt. Fiber Commun. Conf., San Diego, CA, USA, 2008, Paper OThW1.
- [14] K. Xu *et al.*, "OSNR monitoring for NRZ-PSK signals using silicon waveguide two-photon absorption," *IEEE Photon. J.*, vol. 3, no. 5, pp. 968–974, Oct. 2011.
- [15] P. J. Winzer, A. K. Gnauck, C. R. Doerr, M. Magarini, and L. L. Buhl, "Spectrally efficient long-haul optical networking using 112-Gb/s polarization-multiplexed 16-QAM," *J. Lightw. Technol.*, vol. 28, no. 4, pp. 547–556, Feb. 2010.
- [16] L. Cohen, "Generalization of the Wiener-Khinchin theorem," *IEEE Signal Process. Lett.*, vol. 5, no. 11, pp. 292–294, Nov. 1998.
- [17] Z. Huang, J. Qiu, D. Kong, M. Yu, Y. Tian, and J. Wu, "An in-band OSNR monitoring technique based on normalized autocorrelation function," presented at the Asia Commun. Photon. Conf., Wuhan, China, 2016, Paper AF2A-100.
- [18] D. Garipey, S. Searcy, G. He, and S. Tibuleac, "Non-intrusive OSNR measurement of polarization-multiplexed signals with spectral shaping and subject to fiber non-linearity with minimum channel spacing of 37.5GHz," *Opt. Exp.*, vol. 24, no. 18, pp. 268550–26860, 2016.